

# NR2D-containing NMDA receptors mediate tissue plasminogen activator-promoted neuronal excitotoxicity

A Baron<sup>1,2</sup>, A Montagne<sup>1,2</sup>, F Casse<sup>1,2</sup>, S Launay<sup>1,2</sup>, E Maubert<sup>1,2</sup>, C Ali<sup>1,2</sup> and D Vivien<sup>\*,1,2</sup>

Although the molecular bases of its actions remain debated, tissue-type plasminogen activator (tPA) is a paradoxical brain protease, as it favours some learning/memory processes, but increases excitotoxic neuronal death. Here, we show that, in cultured cortical neurons, tPA selectively promotes NR2D-containing *N*-methyl-D-aspartate receptor (NMDAR)-dependent activation. We show that tPA-mediated signalling and neurotoxicity through the NMDAR are blocked by co-application of an NR2D antagonist (phenanthrene derivative (2S<sup>\*</sup>, 3R<sup>\*</sup>)-1-(phenanthrene-2-carbonyl)piperazine-2,3-dicarboxylic acid, PPDA) or knockdown of neuronal NR2D expression. In sharp contrast with cortical neurons, hippocampal neurons do not exhibit NR2D both *in vitro* and *in vivo* and are consequently resistant to tPA-promoted NMDAR-mediated neurotoxicity. Moreover, we have shown that activation of synaptic NMDAR prevents further tPA-dependent NMDAR-mediated neurotoxicity and sensitivity to PPDA. This study shows that the earlier described pro-neurotoxic effect of tPA is mediated by NR2D-containing NMDAR-dependent extracellular signal-regulated kinase activation, a deleterious effect prevented by synaptic pre-activation.

*Cell Death and Differentiation* (2010) 17, 860–871; doi:10.1038/cdd.2009.172; published online 13 November 2009

In the central nervous system, the ability to convert plasminogen to plasmin was the first proposed molecular mechanism of action of tissue-type plasminogen activator (tPA) for not only the control of fibrinolysis, but also of neuronal survival and plasticity.<sup>1–3</sup> However, tPA not only activates plasminogen, but rather acts through several modalities<sup>4</sup> by interacting with the low-density lipoprotein-related receptor protein (LRP),<sup>5–8</sup> annexin-II<sup>9</sup> or *N*-methyl-D-aspartate receptors (NMDAR).<sup>1,10–12</sup> These interactions mediate several potentially damaging effects of tPA, including potentiation of NMDAR-mediated signalling and excitotoxicity.<sup>6,7,10</sup> During excitotoxic conditions, tPA has been shown to promote NMDA-induced calcium influx in cortical neurons and subsequent neuronal death through the binding to and cleavage of the NR1 subunit of the NMDAR, either directly<sup>10,11</sup> or through the recruitment of LRP.<sup>7</sup> The interaction between tPA and the NR1 subunit was shown *in vivo* to be involved in both excitotoxic and memory paradigms in mice.<sup>12</sup> The intimate link between tPA and NMDAR is reinforced by other observations, such as the modulation of the phosphorylation state of the NR2B subunit of the NMDAR in conditions of chronic alcohol consumption and contextual fear conditioning<sup>13,14</sup> or the promotion of NMDAR-dependent extracellular signal-regulated kinase (Erk( $\frac{1}{2}$ )) signalling in hippocampal neurons.<sup>6,15</sup> Thus, there is now accumulating evidence that tPA must be considered as a positive neuromodulator of NMDAR-mediated glutamatergic transmission.<sup>11,16</sup>

NMDAR have a crucial function in brain development, plasticity and survival.<sup>17</sup> Deregulations of these receptors can contribute to a variety of neurological and neurodegenerative disorders.<sup>18,19</sup> NMDAR are mainly composed of assembled NR1a/b and heteromeric NR2 subunits, including NR2A, NR2B and NR2D.<sup>20</sup> Both subunit composition and localization within the neuron (synaptic or extra-synaptic)<sup>21</sup> and subunit-specific protein associations<sup>22</sup> of NMDAR are key determinants of their signalling capacities and implications in the control of neuronal death and survival.

We evidence here that tPA promotes signalling and subsequent neurotoxicity through NR2D subunit-containing NMDAR. In addition, pre-stimulation of synaptic NMDAR prevents tPA-induced potentiation of NR2D-containing NMDAR-dependent Erk( $\frac{1}{2}$ ) activation and subsequent pro-neurotoxicity.

## Results

### tPA exacerbates neurotoxicity through NR2D-containing NMDAR.

Erk( $\frac{1}{2}$ ), a member of the mitogen-activated kinase (MAPK) family, was earlier reported to be recruited in response to NMDAR activation.<sup>15</sup> We thus used phosphorylation of Erk( $\frac{1}{2}$ ) as an index of NMDAR-dependent signalling. Accordingly, in primary cultures of pure cortical neurons maintained either 7 days *in vitro* (DIV) (Supplementary Figure 1a and b) or 12–14 DIV (Supplementary

<sup>1</sup>INSERM, INSERM U919, Serine Proteases and Pathophysiology of the neurovascular Unit (SP2U), Cyceron, University of Caen Basse-Normandie, Caen Cedex F-14074, France and <sup>2</sup>CNRS, UMR CNRS 6232 Ci-NAPs 'Center for imaging – Neurosciences and Application to Pathologies', Cyceron, Caen Cedex F-14074, France  
\*Corresponding author: D Vivien, INSERM U919, Serine Proteases and Pathophysiology of the neurovascular Unit (SP2U), UMR CNRS 6232 Ci-NAPs 'Center of imaging – Neurosciences and Application to Pathologies', Bd H. Becquerel, BP 5229, Caen Cedex F-14074, France. Tel: +332 3147 0166; Fax: +332 3147 0222; E-mail: vivien@cyceron.fr

**Keywords:** NR2D; tPA; NMDA; excitotoxicity; pre-conditioning

**Abbreviations:** 4-AP, 4-aminopyridin; Erk( $\frac{1}{2}$ ), extracellular signal-regulated kinase; LRP, low-density lipoprotein-related receptor protein; NMDAR, *N*-methyl-D-aspartate receptor; PPDA, phenanthrene derivative (2S<sup>\*</sup>, 3R<sup>\*</sup>)-1-(phenanthrene-2-carbonyl)piperazine-2,3-dicarboxylic acid; tPA, tissue-type plasminogen activator  
Received 01.5.09; revised 07.10.09; accepted 07.10.09; Edited by V De Laurenzi; published online 13.11.09

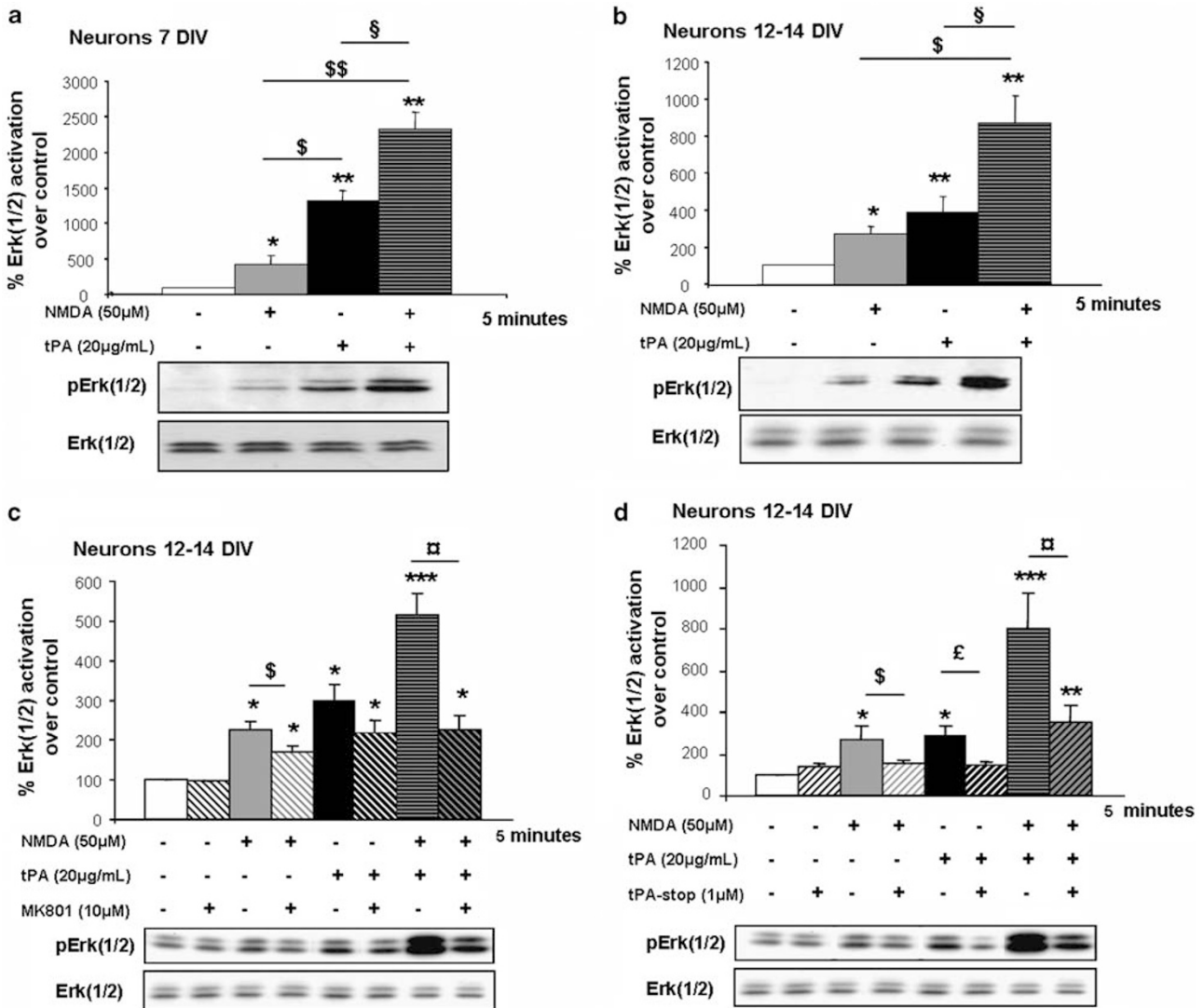


**Figure 1** Catalytic tPA promotes NMDAR-induced Erk(1/2) MAPK activation (a, b). Immunodetection of activated and total Erk(1/2) performed after 5 min of treatment of cortical neurons (7 DIV for a; 12–14 DIV for b) with NMDA (50  $\mu$ M), tPA (20  $\mu$ g/ml) or NMDA(50  $\mu$ M) + tPA(20  $\mu$ g/ml). The graphs show the quantification of Erk(1/2) activation. Data are represented as mean  $\pm$  S.E.M. (N = 8; n = 24) relative to control (\*,  $P < 0.05$ ; \*\*,  $P < 0.01$ ). \*Indicates significantly different from control;  $\S$ indicates significantly different from NMDA treatment;  $\S$ indicates significantly different from tPA treatment. (c, d) Immunodetection of activated and total Erk(1/2) performed after 5 min of treatment of cortical neurons (12–14 DIV) with NMDA (50  $\mu$ M), tPA (20  $\mu$ g/ml) or NMDA (50  $\mu$ M) + tPA (20  $\mu$ g/ml)  $\pm$  MK-801 (10  $\mu$ M) (c) or  $\pm$  tPA-stop (1  $\mu$ M) (d). The graphs show the quantification of Erk(1/2) activation. Data are represented as mean  $\pm$  S.E.M. (N = 4; n = 12) relative to control (\*,  $P < 0.05$ ; \*\*,  $P < 0.01$ ; \*\*\*,  $P < 0.001$ ). \*Indicates significantly different from control;  $\S$ indicates significantly different from NMDA treatment;  $\S$ indicates significantly different from tPA treatment;  $\S$ indicates significantly different from NMDA + tPA treatment

Figure 1c and d), we observed that NMDA (50  $\mu$ M) induced a rapid and transient activation of Erk(1/2) within 5 min, an effect which disappeared as early as after 15 min (Supplementary Figure 1b–d). This activation of Erk(1/2) after 5 min of NMDA exposure was strongly potentiated by tPA (Figure 1a and b). In the presence of MK-801 (10  $\mu$ M), an NMDAR-channel blocker with high affinity and a very slow off rate, Erk(1/2) activation induced by NMDA alone, or NMDA plus tPA (20  $\mu$ g/ml) was dramatically reduced in neurons maintained for 12–14 DIV (Figure 1c), arguing that Erk(1/2) activation is dependent on NMDAR activation. tPA alone also led to an increased activation of Erk(1/2), which was not blocked by the addition of MK-801 (10  $\mu$ M) (Figure 1c), suggesting as shown

earlier<sup>15</sup> that tPA could mediate some of its effects through other receptors.

The serine protease activity of tPA has been shown to be necessary to influence NMDAR-induced calcium influx.<sup>10,11</sup> To determine whether this is also the case for NMDA-induced Erk(1/2) phosphorylation, neurons were treated with tPA-stop (1  $\mu$ M), a synthetic inhibitor of the proteolytic activity of tPA. Exogenously added tPA or released endogenous tPA because of treatment with NMDA<sup>10</sup> both led to increased Erk(1/2) phosphorylation, and in both cases, addition of tPA-stop caused a significant reversal effect (Figure 1d). A proteolytic event is thus necessary for tPA-induced potentiation of NMDAR-induced Erk(1/2) activation.

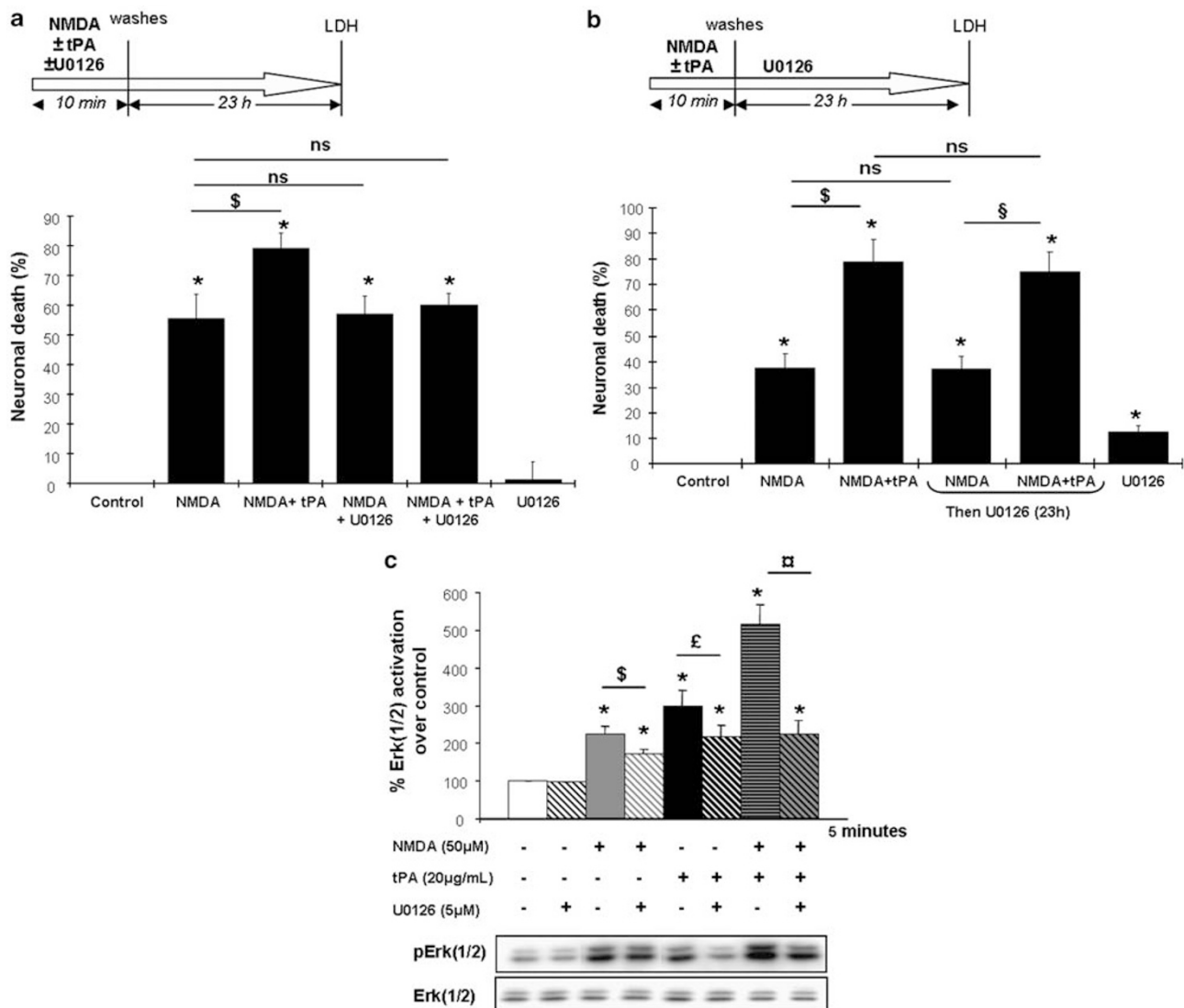


**Figure 2** Important function of Erk(1/2) MAPK activation in the pro-excitotoxic effect of tPA. Neurons (12–14 DIV) were exposed (a) for 10 min to NMDA (50 μM) ± tPA (20 μg/ml) ± U0126 (5 μM), or (b) for 10 min to NMDA (50 μM) ± tPA (20 μg/ml) and then U0126 was added after washes during the last 23 h 50 min. LDH released into the bathing medium was assessed 24 h after the beginning of the excitotoxic exposure. Data are represented as mean ± S.E.M. ( $N = 4$ ;  $n = 16$ ) relative to control (\*,  $S, S, P < 0.05$ ). \*Indicates significantly different from control;  $S$  indicates significantly different from NMDA treatment;  $S$  indicates significantly different from NMDA (10 min) + U0126 (23 h) treatment. (ns: not significant). (c) Immunodetection of activated and total Erk(1/2) performed after 5 min of treatment of cortical neurons (12–14 DIV) in the presence of NMDA (50 μM), tPA (20 μg/ml) or NMDA (50 μM) + tPA (20 μg/ml) ± U0126 (5 μM). The graph shows the quantification of Erk(1/2) activation. Data are represented as mean ± S.E.M. ( $N = 3$ ;  $n = 9$ ) relative to control (\*,  $S, S, P < 0.05$ ). \*Indicates significantly different from control;  $S$  indicates significantly different from NMDA treatment;  $S$  indicates significantly different from tPA treatment;  $S$  indicates significantly different from NMDA + tPA treatment

In agreement with the earlier shown aggravating effect of tPA on slowly triggered NMDA toxicity,<sup>10</sup> we observed that a co-application of tPA (20 μg/ml) during a short exposure (10 min) to a high concentration of NMDA (50 μM) in 12–14 DIV neuronal cultures increased neuronal death measured 24 h later (Figure 2a). To investigate the possible involvement of early Erk(1/2) MAPK activation in this tPA-induced potentiation of NMDAR-mediated neurotoxicity, a co-application of tPA and/or U0126 (5 μM), the upstream MAPK kinase (MEK(1/2)) inhibitor, was performed during the 10 min exposure of neurons to NMDA and neuronal death was measured at 24 h. In such conditions, the blockage of Erk(1/2) MAPK

completely prevented the pro-excitotoxic effect of tPA (Figure 2a) with no effect on NMDA-mediated neuronal death when applied alone. In contrast, when added after this period of 10 min of NMDA/tPA co-treatment, U0126 did not prevent tPA-induced potentiation of NMDA-mediated neurotoxicity (Figure 2b). These data confirm that early Erk(1/2) MAPK activation induced by tPA in the presence of NMDA mediates the pro-neurotoxic effects of tPA. U0126 was also associated with the prevention of the ability of tPA to promote NMDAR-dependent activation of Erk(1/2) signalling (Figure 2c).

Then, the possible involvement of LRP in NMDAR–tPA interaction was investigated by using receptor-associated

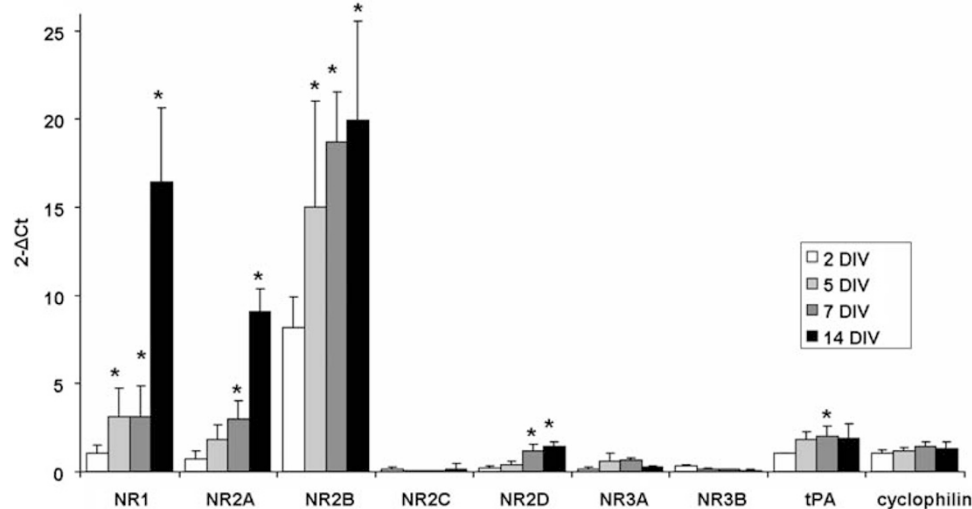


**Figure 3** Characterization of tPA and NR2D expression. mRNA levels of NMDAR subunits (NR1, NR2 and NR3) and tPA in cultured neurons at 2, 5, 7 and 14 DIV ( $N=3$ ,  $n=9$ ). The results of relative levels of mRNA expression were computed by calculating the  $2^{-\Delta Ct}$  and are represented by mean  $\pm$  S.D. \*Indicates significantly different from the 2 DIV value ( $P<0.05$ ). The house keeping gene expression (cyclophilin) was not influenced by the stage *in vitro*

protein (RAP), a competitive antagonist of LRP. Treatment with RAP failed to influence both Erk( $\frac{1}{2}$ ) signalling induced by application of tPA and/or NMDA (Supplementary Figure 2a) and the ability of tPA to promote NMDA-induced neuronal death (Supplementary Figure 2b), ruling out any involvement of LRP on the observed effects of tPA.

When characterizing the temporal profile of NMDAR subunits expression according to the maturation state of primary cultures of cortical neurons (2 to 14 DIV), we found, in addition to an up-regulation of NR1 and NR2A expression during neuronal maturation *in vitro*, a significant over-expression of NR2D subunit (Figure 3). The expression levels of NR2C mRNA were low, whatever the stage investigated may be. A confocal microscopy analysis confirmed the presence of an NR2D and NR1 positive immunostaining at the neuronal membrane (see Figure 8b). We postulated that NR2D could have a critical function in the ability of tPA to promote NMDAR-mediated neurotoxicity. To address this question, we took advantage of the absence of NR2C subunits in our cell culture system (Figure 3) and used phenanthrene derivative (2S\*, 3R\*)-1-(phenanthrene-2-carbonyl)piperazine-2,3-dicarboxylic acid (PPDA) at a concentration of  $0.2 \mu\text{M}$ , earlier reported to inhibit NR2D-containing NMDAR.<sup>23,24</sup> In the presence of PPDA, the deleterious effect of tPA on NMDA-induced neuronal death was completely prevented (Figure 4a), supporting the actual involvement of NR2D-containing NMDAR. To further validate the hypothesis that NR2D subunit has an important function in NMDAR-mediated neurotoxicity, primary cultures of cortical neurons (12–14 DIV) were transiently transfected with Stealth RNA interference targeting NR2D. Among three tested small-interfering RNAs (siRNAs), we selected one (GRIN2D 23) reducing NR2D mRNA expression by 40% (Figure 4b) and having no effect on mRNA levels for the other NMDAR subunits (NR1, NR2A, NR2B, NR2C, NR3A, NR3B) (data not shown). We found that the knockdown of neuronal NR2D expression had no effect on basal NMDA-induced neuronal

death, but prevented the potentiating effect of tPA (Figure 4c). Accordingly, NR2D RNA interference prevented tPA-promoted NMDAR-induced Erk( $\frac{1}{2}$ ) signalling (Figure 4d).

Interestingly, we observed a difference of sensitivity of neurons to the pro-excitotoxic effect of tPA according to their brain structure of origin. Indeed, although tPA was able to potentiate NMDA-dependent neuronal death in cortical cultures (Figure 5A), it failed to do so in hippocampal neurons (Figure 5B). RT-qPCR (Figure 5C), immunocytochemistry and immunohistochemistry (Figure 5D) revealed that while the NR2D subunit is clearly expressed in cortical neurons, it is barely detectable in hippocampal neurons of CA1, CA3 and gyrus dentate areas. Of note, neurons of CA2 exhibit NR2D. On the basis of these observations, we compared the sensitivity of these two brain structures to an intravenous administration of tPA ( $10 \text{ mg/ml}$ ) during an NMDA-induced excitotoxic challenge. As expected, although tPA promoted NMDA-induced cortical injury (Figure 5E and F), it had no effect on the lesion induced by NMDA in the hippocampus (Figure 5G and H). Altogether these data show that NR2D has an important function in tPA-promoted excitotoxicity, which might be of significant relevance for several neurodegenerative disorders, including ischemic brain injury.

**Priming of synaptic NMDAR prevents tPA-promoted NMDAR signalling and neurotoxicity.** The neurotoxic effects of NMDA at a concentration of  $50 \mu\text{M}$  are thought to be mainly attributable to extra-synaptic NMDAR.<sup>25</sup> Accordingly, we sought to determine whether the synaptic NMDAR have any implication in the potentiation of NMDA-dependent signalling and death by tPA. Synaptic NMDAR were specifically activated by application of a combination of bicuculline (a GABA-A inhibitor;  $50 \mu\text{M}$ ) and 4-aminopyridin (4-AP, a weak potassium-channel blocker;  $2.5 \text{ mM}$ ) as described earlier.<sup>25,26</sup> Although bicuculline-induced Erk( $\frac{1}{2}$ ) phosphorylation was prevented by MK-801 (Figure 6a), exogenous tPA failed to influence Erk( $\frac{1}{2}$ ) signalling after

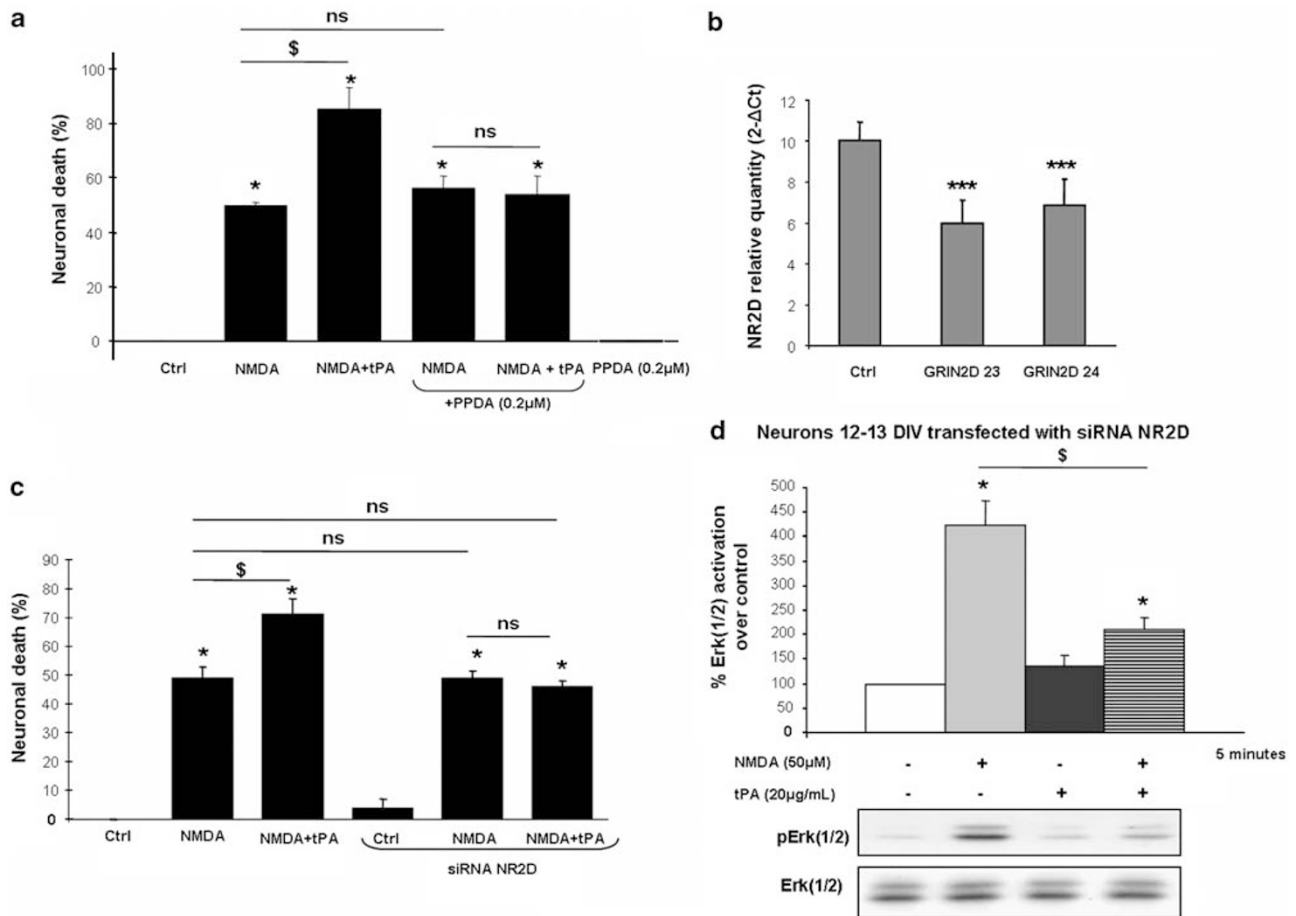


**Figure 4** The tPA promotes NR2D-containing NMDAR signalling and neurotoxicity (a) Neurons (12–14 DIV) were exposed for 60 min to NMDA (50 μM) ± tPA (20 μg/ml). PPDA (0.2 μM) was added concurrently with NMDA to block NR2D-containing NMDAR. LDH released into the bathing medium was assessed 24 h after the excitotoxic exposure. Data are represented as mean ± S.E.M. ( $N=3$ ;  $n=12$ ) relative to control ( $^{*}\text{P}<0.05$ ).  $^{*}$ Indicates significantly different from control;  $^{\$}$ indicates significantly different from NMDA treatment; ns: not significant. (b) mRNA levels of NR2D NMDAR subunits in cultured neurons at 12–13 DIV ( $N=3$ ;  $n=18$ ) were evaluated after transient transfection of neurons with either siRNA GRIN2D 23 or siRNA GRIN2D 24, respectively. Relative levels of mRNA expression were measured by quantitative PCR. The results were computed in relative quantity ( $2^{-\Delta\text{Ct}}$ ). The graph represents mean values ± S.D.  $^{*}$ Indicates significantly different from the control value ( $^{***}\text{P}<0.001$ ). (c) Neurons (12–14 DIV) transfected or not with siRNA GRIN2D 23 were exposed for 60 min to NMDA (50 μM) alone or in the presence of tPA (20 μg/ml). LDH released into the bathing medium was assessed 24 h after the excitotoxic exposure. (d) Immunodetection of activated and total Erk( $\frac{1}{2}$ ) performed after either 5 min of treatment of siRNA GRIN2D 23 transfected neurons (12–3 DIV) in the presence of NMDA (50 μM), tPA (20 μg/ml) and NMDA (50 μM) + tPA (20 μg/ml). The graph shows the quantification of Erk( $\frac{1}{2}$ ) activation in the same conditions as described in (c). For (c, d), data are represented as mean ± S.E.M. ((c)  $N=3$ ;  $n=12$ ; (d)  $N=4$ ;  $n=12$ ) relative to control ( $^{*}\text{P}<0.05$ ).  $^{*}$ Indicates significantly different from control;  $^{\$}$ indicates significantly different from NMDA treatment; ns: not significant

bicuculline + 4-AP exposure in neurons maintained for 12–14 DIV (Figure 6b).

On the basis of these observations, this paradigm was used as a protocol of synaptic preconditioning before NMDA application. Neurons were first treated with bicuculline + 4-AP, followed by addition of MK-801 (10 μM) and subsequent application of NMDA (50 μM) alone or with tPA. Interestingly, in such conditions, while the rapid and transient NMDAR-induced activation of Erk( $\frac{1}{2}$ ) (at 5 min) was not affected, tPA was no longer able to potentiate it (Figure 6c and d). These data show that prior stimulation of synaptic NMDAR could prevent potentiation of NMDAR-dependent Erk( $\frac{1}{2}$ ) signalling by tPA. Accordingly, we observed that, although pre-stimulation and then blockage of synaptic NMDAR did not affect subsequent NMDAR-induced neurotoxicity (around 40% of

neuronal death similar to what was observed after regular application of NMDA), they prevented the ability of tPA to potentiate NMDA-dependent neurotoxicity (Figure 7a). To rule out a potential effect mediated by a direct bicuculline-dependent activation of GABA<sub>A</sub> receptors, additional experiments were performed by using KCl-induced depolarization to stimulate synaptic NMDAR before their blockage by MK-801. Consistent with our earlier observations, although tPA promoted NMDA-induced excitotoxicity, it had no effect when NMDA exposure was preceded by a priming of synaptic NMDAR (Figure 7b). Then, the same experiments were performed without blocking synaptic NMDAR by MK-801. As described above, while the pre-stimulation of synaptic NMDAR (by bicuculline + 4-AP or KCl) did not affect NMDA-dependent neurotoxicity, it prevented the pro-excitotoxic

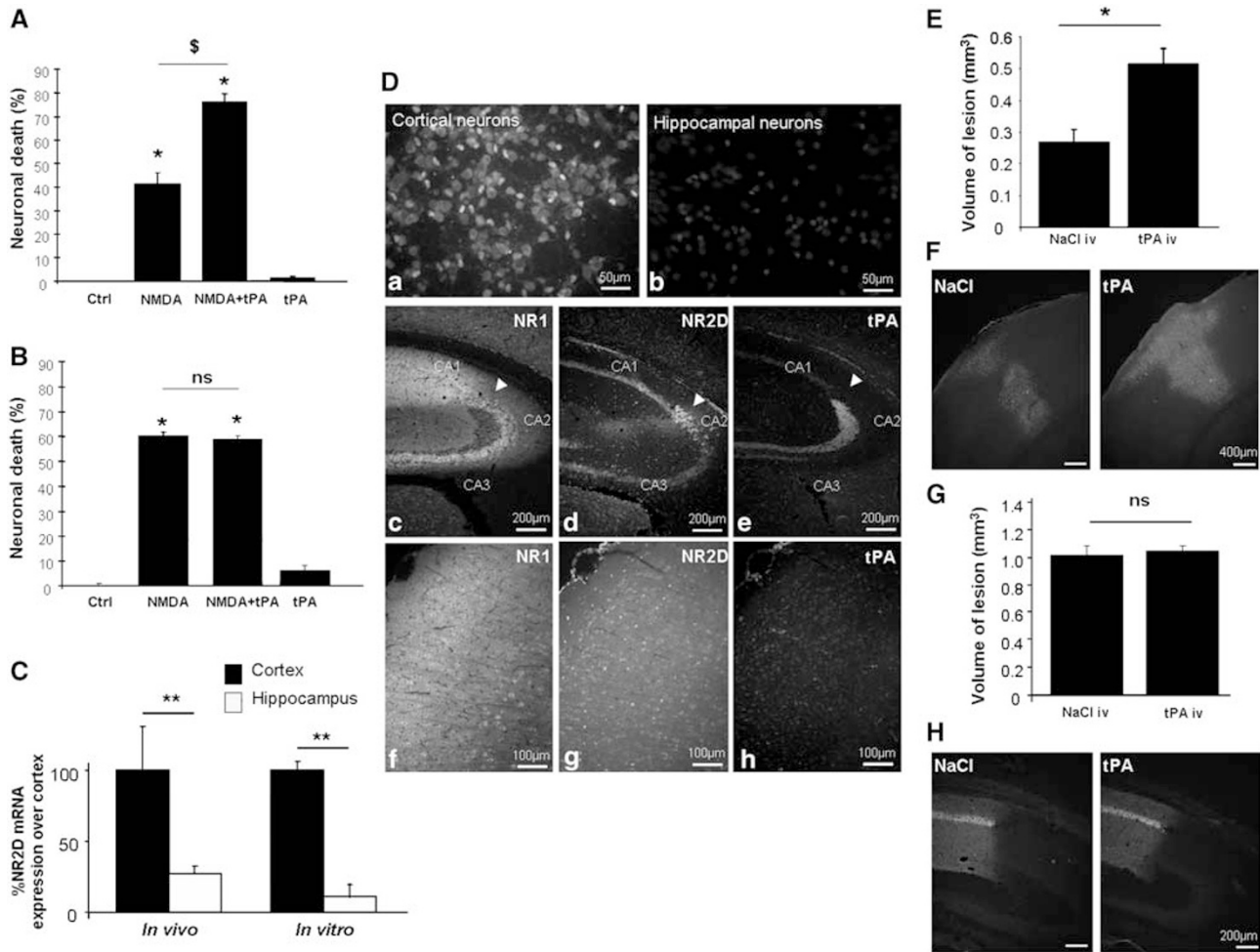


**Figure 5** tPA fails to potentiate excitotoxicity of hippocampal neurons lacking NR2D. (A) Cortical neurons (12–14 DIV) or (B) hippocampal neurons (12–14 DIV) were exposed for 60 min to NMDA (50  $\mu$ M)  $\pm$  tPA (20  $\mu$ g/ml). LDH released into the bathing medium was assessed 24 h after the excitotoxic exposure. Data are represented as mean  $\pm$  S.E.M. ( $N = 3$ ;  $n = 12$ ) relative to control (\*,  $^{\S}P < 0.05$ ). \*Indicates significantly different from control;  $^{\S}$ indicates significantly different from NMDA treatment; ns: not significant ( $N = 6$ ,  $n = 6$ ). (C) mRNA levels of NR2D subunit in cortical or hippocampal extracts and in cultured cortical or hippocampal neurons (14 DIV). The results of relative levels of mRNA expression (%) were expressed over the cortical expression. \*\*Indicates significantly different from the cortical value ( $P < 0.01$ ). (D) Immunostaining for NR2D (green) performed on primary cultures of mouse cortical (a) or hippocampal (b) neurons. (c–h) Immunostaining for NR2D (green) (c, d, f, g) and tPA (red) (e–h) performed from hippocampus (c–e) and cortex (f–h). DAPI staining is in blue. Scale bars represent 50  $\mu$ m for (a, b), 200  $\mu$ m for (c–h). NMDA (2.5 nmoles) was injected either in the cortex (E, F) or in the hippocampus (5 nmoles) (G, H) with or not intravenous injection of tPA (10 mg/kg); 24 h later lesions were stained with Fluoro-Jade C (F–H) and an image analysis system was used to measure the lesioned area (E) cortex; (H) hippocampus). Scale bars represent 400  $\mu$ m for cortex (F) and 200  $\mu$ m for hippocampus (H). Data are represented as mean  $\pm$  S.E.M. ( $N = 4$  for cortex,  $N = 5$  for hippocampus) relative to control (\* $P < 0.05$ ). \*Indicates significantly different from NaCl(iv) treatment; ns: not significant (The colour reproduction of this figure is available on the html full text version of the manuscript)

effect of tPA (Figure 7c and d). Thus, pre-stimulation of synaptic NMDAR prevents potentiation of NMDA-induced signalling and neurotoxicity by tPA. Interestingly, PPDA (used at 1  $\mu$ M, a concentration leading to a reduced NMDA-dependent neurotoxicity) did not influence NMDA-mediated neurotoxicity after a pre-synaptic priming (KCl stimulation as described above) (Figure 8a). Accordingly, immunocytochemistry for NR2D performed in primary cultures of cortical neurons showed that synaptic stimulation induced either by a 1 h exposure to bicuculline + 4-AP or a 15 min application of KCl led to a reduction of NR2D subunits available at the neuronal surface ( $\sim 65$  and  $\sim 50\%$ , respectively) compared with the levels of NR1, which were not modified (Figure 8b and d).

These data suggest that a pre-stimulation of synaptic NMDAR probably leads to a critical change in the distribution

of the NR2D-containing NMDAR that prevents NMDA-mediated neurotoxicity and potentiation by tPA.

## Discussion

It is now well admitted that NMDAR differentially control neuronal outcome depending on either their cellular localization<sup>26</sup> and/or their composition in subunit<sup>27</sup> and/or their anchorage with cytoplasmic or membrane-associated proteins.<sup>22</sup>

In this study, we first show that NMDAR-dependent Erk(1/2) activation is potentiated by both exogenous and endogenous tPA and that its catalytic activity of tPA is a necessary event. These data are in agreement with earlier reports, showing that the proteolytic activity of tPA is critical to mediate its

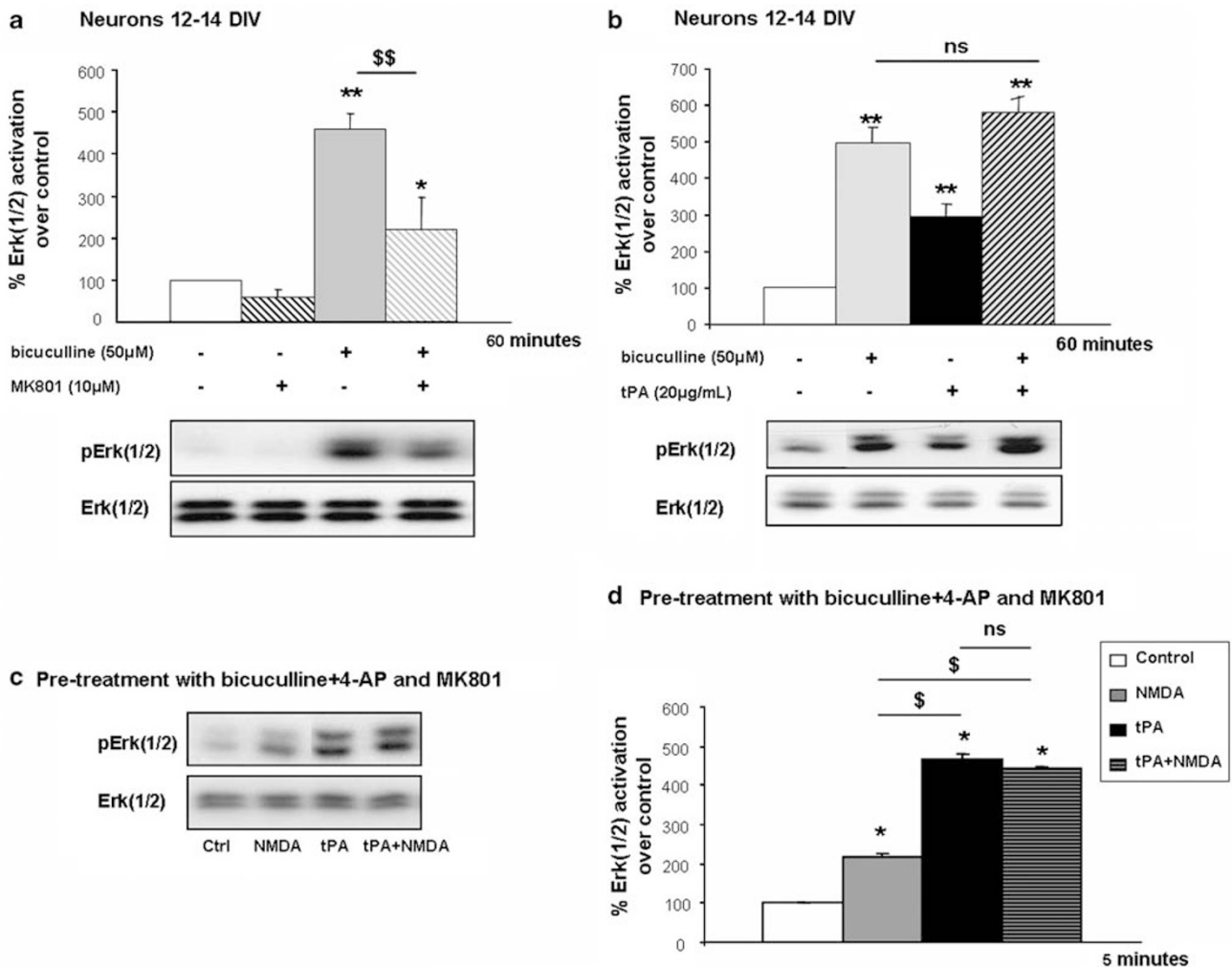


**Figure 6** Synaptic pre-stimulation prevents tPA-promoted NMDAR signalling. (a) Immunodetection of activated and total Erk(1/2) performed after 1 h of treatment of cortical neurons (12–14 DIV) with bicuculline (50 μM) + 4-AP (2.5 mM), ± MK-801 (10 μM). The graph shows the quantification of Erk(1/2) activation. (b) Immunodetection of activated and total Erk(1/2) performed after 1 h of treatment of cortical neurons (12–14 DIV) with bicuculline (50 μM) + 4-AP (2.5 mM), tPA (20 μg/ml) or bicuculline (50 μM) + 4-AP (2.5 mM) + tPA (20 μg/ml). The graph shows the quantification of Erk(1/2) activation. Data are represented as mean ± S.E.M. ( $N=4$ ;  $n=12$ ) relative to control (\* $P<0.05$ ; \*\*,  $^{\S}P<0.01$ ). (a, b) \*indicates significantly different from control;  $^{\S}$ indicates significantly different from bicuculline + 4-AP treatment; ns: not significant. (c) Immunodetection of activated and total Erk(1/2) performed after 5 min of cortical neurons (12–14 DIV) with NMDA (50 μM), tPA (20 μg/ml) or NMDA + tPA after priming. (d) The graph shows the quantification of Erk(1/2) activation. Data are represented as mean ± S.E.M. ( $N=4$ ;  $n=12$ ) relative to control (\*,  $^{\S}P<0.05$ ). \*Indicates significantly different from control;  $^{\S}$ indicates significantly different from NMDA treatment; ns: not significant

pro-neurotoxic effects.<sup>7,10,11</sup> In contrast, others have shown that tPA promotes NMDA-induced Erk(1/2) signalling in hippocampal neurons independently of its proteolytic activity.<sup>15</sup> Whether differences in maturity and/or brain structure of origin can explain this discrepancy remains to be defined. This data did not indicate an involvement of LRP in this mechanism. A recent report<sup>6</sup> suggests that tPA could promote NMDAR signalling through an earlier recruitment of LPR-1 and a possible post-synaptic density-95 (PSD-95)-dependent interaction of tPA bound-LRP-1 with the NR1 subunit of the NMDAR. Surprisingly, although the tPA-induced potentiation of NMDAR signalling was extensively reported, neither co-application of tPA and NMDA were performed nor were neurotoxicity assays performed by these authors. Hence, we cannot exclude that in physiological conditions, a participation

of LRP could occur, a mechanism that could be bypassed in pathological conditions, which cause overactivation of NMDAR. Moreover, in an earlier work,<sup>11</sup> LRP has been described to be involved in the reuptake of tPA by astrocytes, suggesting a possible interference of LRP-dependent mechanism in cultured neurons-containing astrocytes.<sup>7</sup> In this study, the primary cultures of neurons used contain <5% of astrocytes.

Differential action of tPA could be also explained by variation in subunit composition of NMDAR. Indeed, NR2A- or NR2B-containing NMDAR within neurons and/or subunit-specific binding partners have been associated with possible differential signalling pathways including neurotoxicity and survival. However, determination of the relative distribution of different NMDAR populations in tPA effects remained a matter

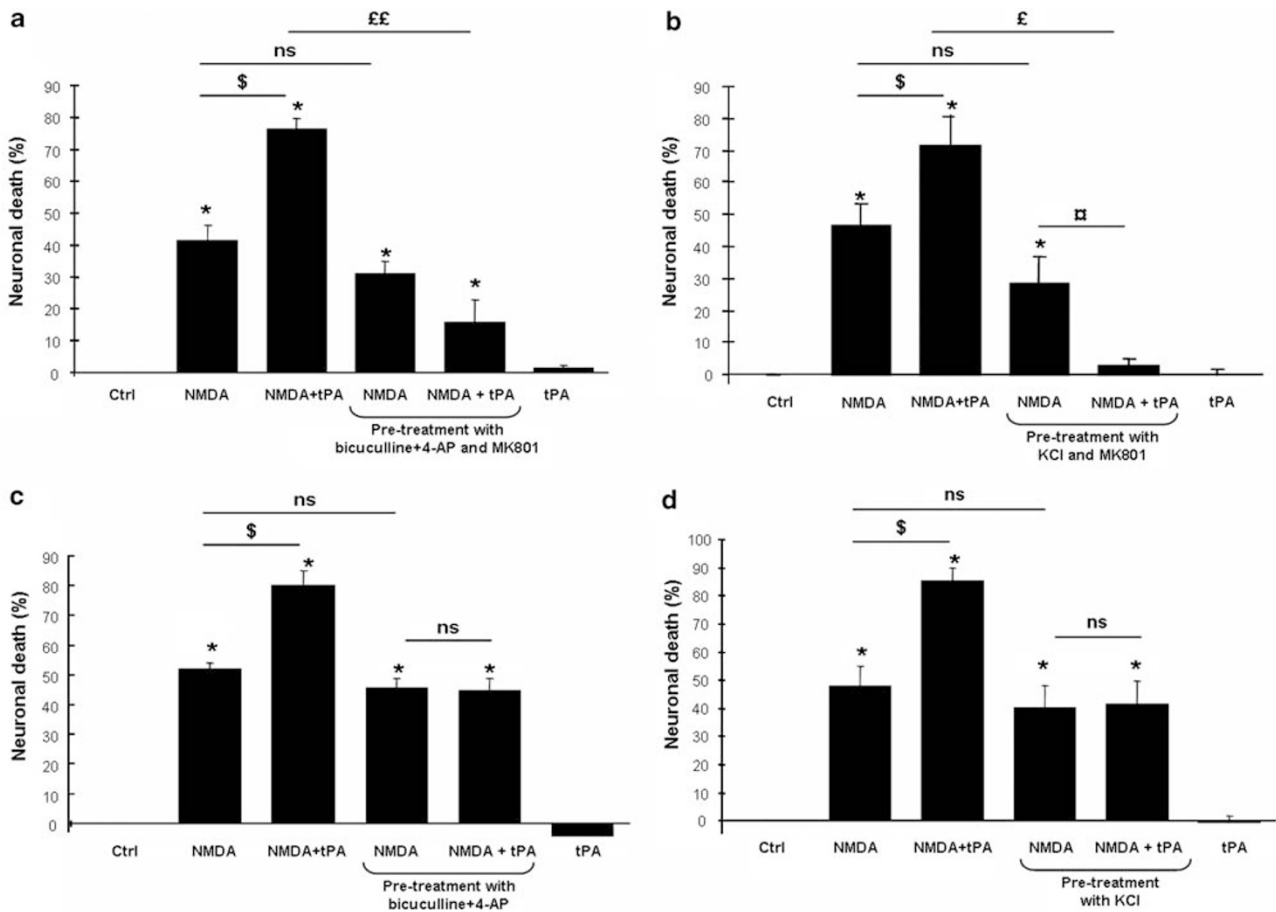


**Figure 7** Pre-stimulation of synaptic NMDAR inhibits NMDAR-mediated neurotoxicity promoted by tPA (a, b). Neurons (12–14 DIV) were subjected or not to an incubation in the presence of either bicuculline (50  $\mu$ M) + 4-AP (2.5 mM) + MK-801 (10  $\mu$ M) (1 h) (a) or KCl (75 mM) + MK-801 (10  $\mu$ M) (15 min) (b), followed by exposure to NMDA (50  $\mu$ M) alone or in the presence of tPA (20  $\mu$ g/ml). LDH released into the bathing medium was assessed after 24 h of treatment. Data are represented as mean  $\pm$  S.E.M. ( $N = 4$ ;  $n = 16$ ) relative to control (\*,  $\$$ ,  $\pounds$ ,  $\boxplus$   $P < 0.05$ ; \*\*,  $\pounds$ ,  $\boxplus$   $P < 0.01$ ). \*Indicates significantly different from control;  $\$$  indicates significantly different from NMDA treatment;  $\pounds$  indicates significantly different from NMDA + tPA treatment;  $\boxplus$  indicates significantly different from NMDA treatment after pre-stimulation; ns: not significant. (c, d) Neurons (12–14 DIV) were subjected or not to an incubation in the presence of either bicuculline (50  $\mu$ M) + 4-AP (2.5 mM) (1 h) (c) or KCl (75 mM; 15 min) (d) prior NMDA (50  $\mu$ M) exposure alone or in the presence of tPA (20  $\mu$ g/ml). LDH released into the bathing medium was assessed 24 h after the excitotoxic exposure. Data are represented as mean  $\pm$  S.E.M. ( $N = 3$ ;  $n = 12$ ) relative to control (\*,  $\$$   $P < 0.05$ ). \*Indicates significantly different from control;  $\$$  indicates significantly different from NMDA treatment; ns: not significant

of debate. Although it is now well admitted that NR1/NR2A and NR1/NR2B di-heteromeric NMDAR are associated with PSD-95, synapse-associated protein 102 (SAP 102) and PSD-93,<sup>28</sup> little is known regarding other NMDAR subunits, especially the NR2D subunit. Interestingly, we found that the NR2D subunit is clearly over-expressed in mature cortical neurons *in vitro* when compared with immature ones. Expression of NR2D subunit was also evidenced *in vivo* in cortical areas of adult mouse brains, in structures showing positive immunostaining for tPA. Accordingly, we postulated that this subunit could contribute to the pro-neurotoxic effect of tPA. PPDA was reported as a selective NR2D competitive antagonist at low concentrations, as we used, with an IC<sub>50</sub> value of around 0.1  $\mu$ M.<sup>23,24,29</sup> Although, PPDA was also reported as an antagonist of NR2C, in agreement with the absence of NR2C mRNA in our cultured cortical neurons, NR2C was only detected in the cerebellum, thalamus and olfactory bulb.<sup>30</sup> At low concentration, PPDA completely

prevented the worsening effect of tPA on NMDA-induced neuronal death. Similarly, a neuronal knockdown of NR2D expression blocked the tPA-dependent potentiation of NMDAR-mediated signalling and neurotoxicity. Although the efficiency of transfection in primary cultures of neurons is rather low, our findings using siRNAs are supported by pharmacological approaches (PPDA) and experiments comparing cortical *versus* hippocampal neurons.

These data are in agreement with recent demonstrations that neurotoxicity is mediated by extra-synaptic NMDAR<sup>26</sup> and that NR2D subunits of NMDAR are exclusively distributed in extra-synaptic NMDAR.<sup>24,31</sup> In support of this, we observed a differential sensitivity of cortical *versus* hippocampal neurons to tPA during excitotoxic conditions that could be explained by the presence and absence, respectively, of the NR2D subunit. Interestingly, the blockage of NMDA-dependent neurotoxicity by a high dose of PPDA disappeared when preceded by pre-synaptic priming. This neuroprotective effect



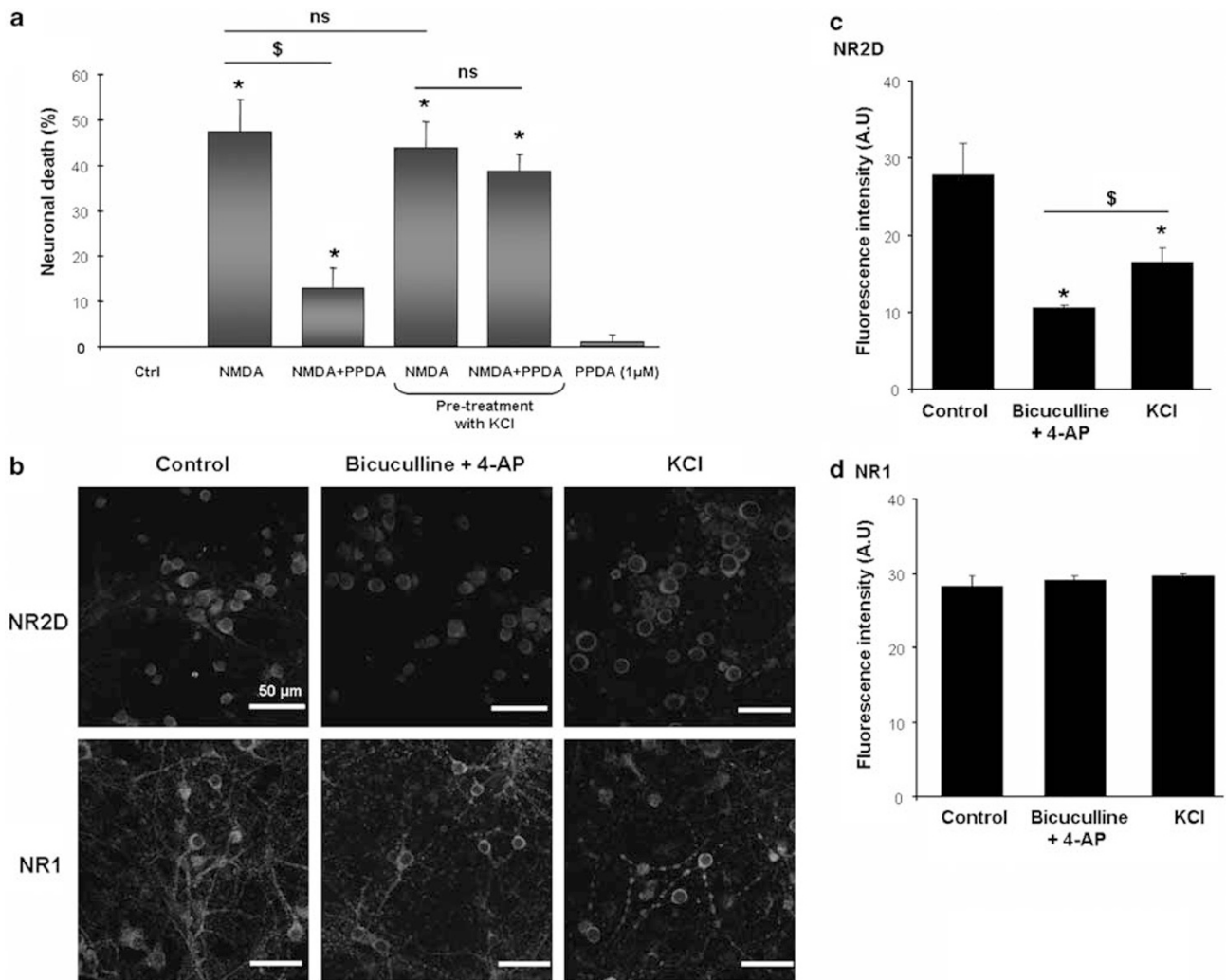


**Figure 8** PPDA does not influence NMDA-mediated neurotoxicity after a pre-synaptic priming. (a) Neurons (12–14 DIV) were subjected or not to a 15 min incubation in the presence of KCl (75 mM), before NMDA (50  $\mu$ M) exposure alone or in the presence of tPA (20  $\mu$ g/ml) for 60 min. PPDA (1  $\mu$ M) was added concurrently to NMDA to block NR2D-containing NMDAR. LDH released into the bathing medium was assessed 24 h after the excitotoxic exposure. Data are represented as mean  $\pm$  S.E.M. ( $N = 3$ ;  $n = 12$ ) relative to control (\*,  $^{\S}P < 0.05$ ). \*Indicates significantly different from control;  $^{\S}$ indicates significantly different from NMDA treatment; ns: not significant. (b) Immunostaining for NR2D (red) performed on primary cultures of mouse cortical neurons after 1 h of bicuculline + 4-AP treatment or 15 min of KCl treatment. Scale bars represent 50  $\mu$ m. (c) NR2D and (d) NR1 immunostaining were quantified by the application of software Meta Imaging Series 6.3. Values are the mean of 45–60 cells ( $N = 3$ ) (A.U.: arbitrary unit). (\*,  $^{\S}P < 0.05$ ). \*Indicates significantly different from control;  $^{\S}$ indicates significantly different from bicuculline + 4-AP treatment (The colour reproduction of this figure is available on the html full text version of the manuscript)

of synaptic pre-stimulation could involve a modification of subunit distribution, in particular of the NR2D subunit. These data are of particular interest and also in agreement with the recent demonstration that extra-synaptic NR2D-containing NMDAR are recruited to the synapse during LTP processes.<sup>24</sup> It is also interesting to note that tPA was earlier reported to promote LTP.<sup>32</sup>

In addition, we show that priming of synaptic NMDAR signalling prevented both tPA-promoted NMDAR activation of Erk(1/2) signalling and subsequent neuronal death. These data could be related to earlier observations that ischemic preconditioning induced either by short exposure to hypoxia or short ischemic episodes could have neuroprotective effects.<sup>33</sup> Moreover, Tauskela *et al.*<sup>34</sup> recently showed that

a synaptic NMDAR preconditioning induces a tolerance to oxygen glucose deprivation. Similarly, a protective function of NMDAR in survival of cultured rat cerebellar granule neurons in the presence of depolarizing concentrations of KCl was earlier proposed.<sup>35</sup> As this treatment was suggested to mimic endogenous NMDAR-mediated glutamate signalling, it was hypothesized that NMDAR were required for neuronal survival. Indeed, low doses of NMDA pre-treatment were reported to protect neurons against cell death induced by glutamate.<sup>25,36</sup> Also relevant to this data, increased synaptic activity induced in cortical cultures protects neurons against neurotoxin in an NMDAR-dependent manner.<sup>26,37</sup> Although in the presence of MK-801, tPA reduced neurotoxicity induced by NMDA after a pre-treatment with Bic + 4-AP, it had no

neuroprotective activity in the absence of MK-801. As MK-801-induced blockage of basal NMDAR signalling was earlier shown to induce apoptotic neuronal death,<sup>38</sup> we can postulate that in such conditions, tPA could display a neurotrophic activity, which fits well with its earlier shown non-proteolytic anti-apoptotic effect.<sup>39</sup>

In pathological scenarios such as ischemia, Ca<sup>2+</sup> influx through the NMDAR is a key mediator of cell death. However, physiological levels of NMDAR activity can promote neuronal survival and resistance to trauma and have important functions in synaptic plasticity and transmission. Here, we show that, although tPA promotes NMDAR-dependent Erk(1/2) signalling and neurotoxicity, priming induced by synaptic NMDAR stimulation completely prevents these effects of tPA. Interestingly, this data also show that NR2D-containing NMDAR are critical effectors of the tPA-mediated neurotoxicity. Altogether, these insights may lead to better therapeutic strategies that could enable selective blockade of pro-death signalling properties of tPA while sparing physiological signalling to survival and plasticity. These data throw a new light on the mechanism by which tPA (endogenous and exogenous) could influence the outcome after stroke. Indeed, although tPA is the only approved treatment for acute stroke because of its thrombolytic properties, blockage of the excitotoxic neuronal damages produced by tPA is now considered as a challenging strategy to improve the efficiency and/or therapeutic window of stroke acute treatment.

## Materials and Methods

**Materials.** NMDA, MK801 and PPDA were purchased from Tocris (Bristol, UK). Human tPA (Actilyse) was purchased from Boehringer Ingelheim (Paris, France). RAP was from Gentaur (Paris, France). tPA-stop was purchased from American Diagnostica (Greenwich, Connecticut). Dulbecco's modified Eagle's medium (DMEM), poly-D-lysine, laminin, glutamine, cytosine  $\beta$ -D-arabinoside, protease inhibitor cocktail, phosphatase inhibitor cocktail, bicuculline, 4-amimopyridin and U0126 ethanolate were purchased from Sigma-Aldrich (L'Isle d'Abeau, France).

**Neuronal cultures.** Neuronal cultures were prepared from foetal mice (embryonic day 15–16) as described earlier.<sup>40</sup> Cortices or hippocampi were dissected and dissociated in DMEM, and plated, respectively, on 24- and 48-well plates earlier coated with poly-D-lysine (0.1 mg/ml) and laminin (0.02 mg/ml). Cells were cultured in DMEM supplemented with 5% fetal bovine serum (Invitrogen, Cergy Pontoise, France), 5% horse serum (Invitrogen) and 2 mM glutamine. Cultures were maintained at 37 °C in a humidified 5% CO<sub>2</sub> atmosphere. Cytosine  $\beta$ -D-arabinoside (10  $\mu$ mol/l) was added after 3 DIV to inhibit glial proliferation. Various treatments were performed after 7 or 12–14 DIV as required.

**Assessment of NMDAR-dependent signalling.** Erk(1/2) activation by phosphorylation was used as an index of NMDAR activity. Synaptic NMDARs were activated by exposure of the primary neuronal cultures to bicuculline (50  $\mu$ M) and 4-AP (2.5 mM) during 1 h. At the indicated times, cells were chilled on ice and lysed in buffer containing Tris-NaCl-Triton 1% of protease inhibitor cocktail and 1% of phosphatase inhibitor cocktail. Lysates were clarified by centrifugation at 13 000  $\times$  g for 10 min at 4 °C. Proteins were quantified by bicinchoninic acid protein assay (Pierce, Thermo Fisher Scientific, Brebières, France) and processed for immunoblotting.

**Immunoblotting.** Protein samples (20  $\mu$ g) were resolved on a 10% SDS-polyacrylamide gel and transferred onto a polyvinylidene difluoride (PVDF) membrane. Membranes were blocked with 5% dried milk in Tris-buffered saline containing 0.05% Tween-20 and incubated with primary antibodies (anti-phosphorylated Erk(1/2), d1/1000; Cell Signalling, Ozyme, Saint Quentin en Yvelines, France). After incubation with the corresponding secondary peroxidase-conjugated streptavidine reagent, proteins were visualized with an enhanced

chemiluminescence ECL Plus immunoblotting detection system (Perkin Elmer-NEN, Paris, France). Total Erk(1/2) levels (d1/1000; Cell Signalling) were investigated either after stripping of the PVDF membranes used for p-ERK or by running separated immunoblots from the same protein extracts.

**Excitotoxic neuronal death.** Excitotoxicity was induced by exposure to NMDA (50  $\mu$ M) in serum-free DMEM supplemented with 10  $\mu$ M of glycine (MS-glycine) for 10 min or 1 h. Wherever mentioned, tPA and inhibitors were co-applied with NMDA. Neuronal death was quantified 24 h later by measurement of the activity of the lactate dehydrogenase (LDH) released from damaged cells into the bathing medium with a cytotoxicity detection kit (Roche Diagnostics, Mannheim, Germany). The LDH level corresponding to the maximal neuronal death was determined in sister cultures exposed to 200  $\mu$ M NMDA (LDH<sub>max</sub>). Background LDH levels were determined in sister cultures subjected to control washes (LDH<sub>min</sub>). Experimental values were measured after subtracting LDH<sub>min</sub> and then normalized to LDH<sub>max</sub>-LDH<sub>min</sub> to express the results in percentage of neuronal death.

**Protocol for priming before NMDAR activation.** Synaptic NMDAR were activated by exposure of neuronal cultures (14 DIV) to bicuculline (50  $\mu$ M), 4-AP (2.5 mM) (1 h) or KCl (75 mM, 15 min) and were simultaneously blocked or not by addition of MK-801 (10  $\mu$ M). Then, neurons were washed with MS-glycine (serum-free DMEM supplemented with 10  $\mu$ M of glycine), and after 1 h, NMDAR were activated by exposure to NMDA (50  $\mu$ M).

**Extraction of total RNA.** Total RNAs were extracted from cultured cells or tissues by using the NucleoSpin RNA II kit from Macherey-Nagel. The samples were lysed in RA1 buffer containing 1% of  $\beta$ -mercaptoethanol. After filtration of the lysates on Nucleospin filter units, total RNAs were purified on Nucleospin RNA II columns according to the manufacturer's instructions and eluted with RNase-free water.

**Quantitative real-time RT-PCR.** One microgram of total RNAs from each sample was reverse transcribed using the Promega RT system (Promega, Charbonnières, France; reverse transcription: 42 °C for 1 h). Two primers were designed for each gene using the Beacon Designer software (Bio-Rad, Marnes-la-Coquette, France). Primer alignments were performed with the BLAST database to ensure the specificity of primers.

NMDA1 forward	CTCTAGCCAGGTCTACGCTATCC	NMDA1 reverse	GACGGGGATCTCTGAGAAGCCA
NMDA2a forward	ACATCCAGGTTCTCCAGTTGG	NMDA2a reverse	GACATGCCAGTCATAGCTCTGC
NMDA2b forward	CCAGAGTGAGAGATGGATTGC	NMDA2b reverse	TGGGCTCAGGGATGAAACTGT
NMDA2d forward	CTGTGTGGTGATGATGTTCTGT	NMDA2d reverse	GTGAAGGTAGAGCCTCCGGG
NMDA2e forward	GGGCTTCTGCATCGACATCC	NMDA2e reverse	ATCATACCATTCCACACCCAGC
NMDA3a forward	ATCCTCAAGCGCATCGGACA	NMDA3a reverse	CGACTCGGCTATCCCTCTGT
NMDA3b forward	GGCCGTGACCAGTTCAGTA	NMDA3b reverse	CAATGGGTGAGGCTGTATCTCG
tPA forward	CTCCGACCCATGCTCAGAA	tPA reverse	TTGTACCAGGCCGCTGTTG
Cyclophilin forward	CAGGGTGGTGACTTTACACGC	Cyclophilin reverse	TGTTGGTCCAGCATTTGCCA

PCR solutions were prepared with RNase-free water containing primers and IQ SYBR Green Supermix (Bio-Rad). For PCR amplification, 20  $\mu$ l of mix were added to 5  $\mu$ l of reverse transcription reaction diluted earlier (1 : 20). Two negative controls were performed during each experiment. In the first control, we used samples without reverse transcription as a template to control contamination of RNA with genomic DNA. In the second control, we used RNase-free water instead of cDNA to prove that qPCR mixes were not contaminated with DNA. Assays were run in triplicate on the iCycler iQ real-time PCR detection system (Bio-Rad). The amplification conditions were as follows: Hot Goldstar enzyme activation, 95 °C for 3 min; 50 cycles of PCR at 95 °C, 15 s and 60 °C, 1 min. The levels of expression of interest gene were computed as follows: relative mRNA expression = 2<sup>-(Ct of gene of interest)</sup>, where Ct is the threshold cycle value.

**RNA interference.** Three Stealth siRNA duplex oligoribonucleotides against NR2D subunits (Invitrogen) were tested. The sequences were as follows: GRIN2D 25 Sense 5'-UGGUAAACCCGUCACUGGUAGUCAU-3', Antisense 5'-AUGACUA CCAGUCACGGGUUACCA-3'; GRIN2D 23 Sense 5'-CCAUCGGUUUCAGCU AUGACCUCUA-3', Antisense 5'-UAGAGUCAUAGCUGAAACCGAUGG-3';

GRIN2D 24 Sense 5'-GCCGUAUCUUUCUUGCCAGCUAUA-3', Antisense 5'-UAUAGCUGGCAAGAAAGAUGACGGC-3'

siRNA oligos (40 nM) were transfected into primary cortical cultures of neurons maintained 10–11 DIV by using a modified protocol in the presence of Lipofectamine 2000 (2  $\mu$ g) (Invitrogen). The Stealth RNA negative Control Duplexes (Invitrogen) that is not homologous to any known genes was used as transfection efficiency detector and a negative control to ensure against induction of non-specific cellular events caused by introduction of the oligoribonucleotides into cells. The Stealth siRNA/lipofectamine complexes were applied during 6 h. Cultures were replaced with MS-glycine after the transfection and cells were treated 48 h later. After characterization by qPCR, among the three siRNA oligo duplexes against NR2D subunit, we selected the one that presents the most significant knockdown effect (GRIN 23; 40% of reduction).

**In vivo excitotoxic lesions.** Male Swiss mice (20–24 g; CERJ, Paris, France) were housed in a temperature-controlled room on a 12-h light/12-h dark cycle with food and water *ad libitum*. Experiments were performed in accordance with French ethical laws (act no. 87–848; Ministère de l'Agriculture et de la Forêt) and European Communities Council Directives of 24 November 1986 (86/609/EEC) guidelines for the care and use of laboratory animals. Animals were deeply anesthetized with isoflurane 5% and, thereafter, maintained with 2.5% isoflurane in a 70%/30% mixture of N<sub>2</sub>O/O<sub>2</sub>. Rectal temperature was maintained at 37  $\pm$  0.5  $^{\circ}$ C throughout the surgical procedure using a feedback-regulated heating system. A catheter was inserted into the tail vein, then excitotoxic lesions were performed. Hippocampal or cortical bilateral injections (coordinates: –2.3 mm posterior, –1.8 mm lateral, –1.1 mm ventral or – coordinates: 0.5 mm posterior,  $\pm$  3.0 mm lateral, –0.8 mm ventral to the bregma, respectively) of NMDA (cortex: 2.5 nmoles; hippocampus: 5 nmoles; total volume of 0.33  $\mu$ l) versus phosphate-buffered saline (PBS) (pH 7.4; total volume 0.33  $\mu$ l) were performed after placing the animals under a stereotaxic frame. Solutions were injected by the use of a micropipette made with hematologic micropipettes (calibrated at 15 mm/ $\mu$ l; assistant ref 555/5; Hecht, Sondheim-Rhoen, Germany). The needle was removed 3 min later. Finally, 200  $\mu$ l bolus intravenous injections of tPA (10 mg/kg) or saline were performed after intracerebral injections.

**Histological analysis of lesion volume.** After 24 h, mice were anesthetized and transcardially perfused with cold heparinized saline (15 ml) followed by 150 ml of fixative (sodium phosphate buffer 0.1 M, pH 7.4 containing 2% paraformaldehyde and 0.2% picric acid). Brains were frequently rinsed in a coons buffer containing 20% sucrose before freezing in Tissue-Tek (Miles Scientific, Naperville, IL, USA). Cryostat-cut coronal brain sections (10  $\mu$ m) were collected and stained with Fluoro-Jade C. Regions of interest were determined through the use of a stereotaxic atlas for the mouse and an image analysis system (MetaVue software, Molecular Devices, Downingtown, PA, USA) was used to measure the lesioned area. The results are expressed as mean  $\pm$  S.E.M.

**Immunocytochemistry and immunohistochemistry.** Neuronal cultures were prepared on four-well Labtek Chamber-Slide culture system (Thermo Fisher Scientific, Rochester, NY, USA) or glass bottom Petri dishes (MatTek corporation, Ashland, MA, USA) earlier coated with poly-D-lysine (0.1 mg/ml) and laminin (0.02 mg/ml). Neurons (14 DIV) were fixed during 30 min with 4% of paraformaldehyde in PBS (0.1 M, pH 7.4). After washes with PBS, they were incubated in the presence of goat polyclonal anti-NR2D or goat polyclonal anti-NR1 (1 : 500; Santa Cruz Biotechnology, Heidelberg, Germany), before an overnight incubation with the secondary antibody F(ab)<sup>2</sup> fragments of donkey anti-Goat IgG linked to tetramethyl rhodamine isothiocyanate (TRITC) (1 : 300, Jackson ImmunoResearch, West Grove, PA, USA). Images were digitally captured using a Nikon Eclipse (TE2000-E) inverted C1 confocal microscope equipped with an oil immersion Nikon  $\times$  60 objective.

Anesthetized (500 mg/kg of choral hydrate) adult Swiss mice were transcardially perfused with cold heparinized saline (15 ml) followed by 150 ml of fixative (PBS 0.1 M, pH 7.4 containing 2% paraformaldehyde and 0.2% picric acid). Cryo-microtome-cut sections (8–12  $\mu$ m) were collected and stored at –80  $^{\circ}$ C. Sections were incubated in the presence of rabbit polyclonal anti-mouse tPA (1 : 3000; from Pr. Carmeliet, University of Leuven, Belgium) and goat polyclonal anti-NR2D (1 : 500) before an overnight incubation with the secondary antibodies, respectively, F(ab)<sup>2</sup> fragments of donkey anti-rabbit IgG linked to TRITC and F(ab)<sup>2</sup> fragments of donkey anti-Goat IgG linked to FITC (Jackson ImmunoResearch).

LabTek and sections were coverslipped with antifade medium containing DAPI. Images were digitally captured using a Leica DM6000 microscope-coupled coolsnap.

Quantification of immunostaining were performed by using the application software Meta Imaging 6.3.

**Statistical analysis.** The results are expressed as the mean  $\pm$  S.E.M. Statistical analyses were performed by the Kruskal–Wallis' test, followed by *post hoc* comparisons, with the Mann–Whitney's test.

### Conflict of interest

The authors declare no conflict of interest.

**Acknowledgements.** We thank Pr Peter Carmeliet for providing us the rabbit polyclonal anti-mouse tPA. We are also grateful to Dr. Alahari for her critical reading of the manuscript. This work was supported by grants from the INSERM and Regional Council of Lower Normandy.

- Baranes D, Lederlein D, Huang YY, Chen M, Bailey CH, Kandel ER. Tissue plasminogen activator contributes to the late phase of LTP and to synaptic growth in the hippocampal mossy fiber pathway. *Neuron* 1998; **21**: 813–825.
- Pang PT, Teng HK, Zaitsev E, Woo NT, Sakata K, Zhen S *et al*. Cleavage of proBDNF by tPA/plasmin is essential for long-term hippocampal plasticity. *Science* 2004; **306**: 487–491.
- Bruno MA, Cuervo AC. Activity-dependent release of precursor nerve growth factor, conversion to mature nerve growth factor, and its degradation by a protease cascade. *Proc Natl Acad Sci USA* 2006; **103**: 6735–6740.
- Yepes M, Roussel BD, Ali C, Vivien D. Tissue-type plasminogen activator in the ischemic brain: more than a thrombolytic. *Trends Neurosci* 2009; **32**: 48–55.
- Benchenane K, Berezowski V, Ali C, Fernández-Monreal M, López-Atalaya JP, Brillault J *et al*. Tissue-type plasminogen activator crosses the intact blood-brain barrier by low-density lipoprotein receptor-mediated protein-mediated transcytosis. *Circulation* 2005; **111**: 2241–2249.
- Martin AM, Kuhlmann C, Trossbach S, Jaeger S, Waldron E, Roebroek A *et al*. The functional role of the second NPXY motif of the LRP1 beta-chain in tissue-type plasminogen activator-mediated activation of N-methyl-D-aspartate receptors. *J Biol Chem* 2008; **283**: 12004–12013.
- Samson AL, Nevin ST, Croucher D, Niego B, Daniel PB, Weiss TW *et al*. Tissue-type plasminogen activator requires a co-receptor to enhance NMDA receptor function. *J Neurochem* 2008; **107**: 1091–1101.
- Polaravaru R, Gongora MC, Yi H, Ranganathan S, Lawrence DA, Strickland D *et al*. Tissue-type plasminogen activator-mediated shedding of astrocytic low-density lipoprotein receptor-related protein increases the permeability of the neurovascular unit. *Blood* 2007; **109**: 3270–3278.
- Lee HY, Hwang IY, Im H, Koh JY, Kim YH. Non-proteolytic neurotrophic effects of tissue plasminogen activator on cultured mouse cerebrocortical neurons. *J Neurochem* 2007; **101**: 1236–1247.
- Nicole O, Docagne F, Ali C, Margail I, Carmeliet P, MacKenzie ET *et al*. The proteolytic activity of tissue-plasminogen activator enhances NMDA receptor-mediated signaling. *Nat Med* 2001; **7**: 59–64.
- Fernández-Monreal M, López-Atalaya JP, Benchenane K, Cacquevel M, Dulin F, Le Caer JP *et al*. Arginine 260 of the amino-terminal domain of NR1 subunit is critical for tissue-type plasminogen activator-mediated enhancement of N-methyl-D-aspartate receptor signaling. *J Biol Chem* 2004; **279**: 50850–50856.
- Benchenane K, Castel H, Boulouard M, Bluthé R, Fernandez-Monreal M, Roussel BD *et al*. Anti-NR1 N-terminal-domain vaccination unmasks the crucial action of tPA on NMDA-receptor-mediated toxicity and spatial memory. *J Cell Sci* 2007; **120**: 578–585.
- Pawlak R, Melchor JP, Matys T, Skrzypiec AE, Strickland S. Ethanol-withdrawal seizures are controlled by tissue plasminogen activator via modulation of NR2B-containing NMDA receptors. *Proc Natl Acad Sci USA* 2005; **102**: 443–448.
- Norris EH, Strickland S. Modulation of NR2B-regulated contextual fear in the hippocampus by the tissue plasminogen activator system. *Proc Natl Acad Sci USA* 2007; **104**: 13473–13478.
- Medina MG, Ledesma MD, Domínguez JE, Medina M, Zafra D, Alameda F *et al*. Tissue plasminogen activator mediates amyloid-induced neurotoxicity via Erk1/2 activation. *EMBO J* 2005; **24**: 1706–1716.
- Samson AL, Medcalf RL. Tissue-type plasminogen activator: a multifaceted modulator of neurotransmission and synaptic plasticity. *Neuron* 2006; **50**: 673–678.
- Thomas GM, Hagan RL. MAPK cascade signalling and synaptic plasticity. *Nat Rev Neurosci* 2004; **5**: 173–183.
- Gardoni F, Di Luca M. New targets for pharmacological intervention in the glutamatergic synapse. *Eur J Pharmacol* 2006; **545**: 2–10.

19. Lau CG, Zukin RS. NMDA receptor trafficking in synaptic plasticity and neuropsychiatric disorders. *Nat Rev Neurosci* 2007; **8**: 413–426.
20. Cull-Candy SG, Leszkiewicz DN. Role of distinct NMDA receptor subtypes at central synapses. *Sci STKE* 2004; **2004**: re16.
21. Papadia S, Hardingham GE. The dichotomy of NMDA receptor signaling. *Neuroscientist* 2007; **13**: 572–579.
22. Kohr G. NMDA receptor function: subunit composition versus spatial distribution. *Cell Tissue Res* 2006; **326**: 439–446.
23. Feng B, Tse HW, Skifter DA, Morley R, Jane DE, Monaghan DT. Structure-activity analysis of a novel NR2C/NR2D-preferring NMDA receptor antagonist: 1-(phenanthrene-2-carbonyl) piperazine-2,3-dicarboxylic acid. *Br J Pharmacol* 2004; **141**: 508–516.
24. Harney SC, Jane DE, Anwyl R. Extrasynaptic NR2D-containing NMDARs are recruited to the synapse during LTP of NMDAR-EPSCs. *J Neurosci* 2008; **28**: 11685–11694.
25. Soriano FX, Papadia S, Hofmann F, Hardingham NR, Bading H, Hardingham GE. Preconditioning doses of NMDA promote neuroprotection by enhancing neuronal excitability. *J Neurosci* 2006; **26**: 4509–4518.
26. Hardingham GE, Fukunaga Y, Bading H. Extrasynaptic NMDARs oppose synaptic NMDARs by triggering CREB shut-off and cell death pathways. *Nat Neurosci* 2002; **5**: 405–414. Comment in: *Nat Neurosci* 2002; **5**: 389–390.
27. Liu Y, Wong TP, Aarts M, Rooyackers A, Liu L, Lai TW *et al*. NMDA receptor subunits have differential roles in mediating excitotoxic neuronal death both *in vitro* and *in vivo*. *J Neurosci* 2007; **27**: 2846–2857.
28. Al-Hallaq RA, Conrads TP, Veenstra TD, Wenthold RJ. NMDA di-heteromeric receptor populations and associated proteins in rat hippocampus. *J Neurosci* 2007; **27**: 8334–8343.
29. Hrabetova S, Serrano P, Blace N, Tse HW, Skifter DA, Jane DE *et al*. Distinct NMDA receptor subpopulations contribute to long-term potentiation and long-term depression induction. *J Neurosci* 2000; **20**: RC81.
30. Wenzel A, Fritschy JM, Mohler H, Benke D. NMDA receptor heterogeneity during postnatal development of the rat brain: differential expression of the NR2A, NR2B, and NR2C subunit proteins. *J Neurochem* 1997; **68**: 469–478.
31. Brickley SG, Misra C, Mok MH, Mishina M, Cull-Candy SG. NR2B and NR2D subunits coassemble in cerebellar Golgi cells to form a distinct NMDA receptor subtype restricted to extrasynaptic sites. *J Neurosci* 2003; **23**: 4958–4966.
32. Pang PT, Teng HK, Zaitsev E, Woo NT, Sakata K, Zhen S *et al*. Cleavage of proBDNF by tPA/plasmin is essential for long-term hippocampal plasticity. *Science* 2004; **306**: 487–491.
33. Zhang J, Qian H, Zhao P, Hong SS, Xia Y. Rapid hypoxia preconditioning protects cortical neurons from glutamate toxicity through delta-opioid receptor. *Stroke* 2006; **37**: 1094–1099.
34. Tauskela JS, Fang H, Hewitt M, Brunette E, Ahuja T, Thiverge JP *et al*. Elevated synaptic activity preconditions neurons against an *in vitro* model of ischemia. *J Biol Chem* 2008; **283**: 34667–34676.
35. Yan GM, Ni B, Weller M, Wood KA, Paul SM. Depolarization or glutamate receptor activation blocks apoptotic cell death of cultured cerebellar granule neurons. *Brain Res* 1994; **656**: 43–51.
36. Marini AM, Paul SM. N-methyl-D-aspartate receptor-mediated neuroprotection in cerebellar granule cells requires new RNA and protein synthesis. *Proc Natl Acad Sci USA* 1992; **89**: 6555–6559.
37. Papadia S, Stevenson P, Hardingham NR, Bading H, Hardingham GE. Nuclear Ca<sup>2+</sup> and the cAMP response element-binding protein family mediate a late phase of activity-dependent neuroprotection. *J Neurosci* 2005; **25**: 4279–4287.
38. Terro F, Esclaire F, Yardin C, Hugon J. N-methyl-D-aspartate receptor blockade enhances neuronal apoptosis induced by serum deprivation. *Neurosci Lett* 2000; **278**: 149–152.
39. Liot G, Roussel BD, Lebeurrier N, Benchenane K, López-Atalaya JP, Vivien D *et al*. Tissue-type plasminogen activator rescues neurones from serum deprivation-induced apoptosis through a mechanism independent of its proteolytic activity. *J Neurochem* 2006; **98**: 1458–1464.
40. Rose K, Goldberg MP, Choi DW. Cytotoxicity in murine cortical cell culture In: Tyson CA, Frazier JM (eds). *In Vitro Biological Methods*. Academic Press: San Diego, California, USA, 1993.

Supplementary Information accompanies the paper on Cell Death and Differentiation website (<http://www.nature.com/cdd>)